Ultrashort Baseline Positioning System: Implementation and Tests at Sea

João N. Picão
(jnpicao@hotmail.com)

Instituto Superior Técnico
Lisboa, Portugal

Abstract

This work presents the design, implementation, and validation at sea of an USBL acoustic positioning system.

A carefully selected acoustic signal emitted from a moving platform is received on an array of hydrophones and is detected, based on a matched filter. Then it is possible to determine the time of arrival (TOA) and to estimate the position of the emitter. The system performance relies on the accurate detection of the expected signal, which may be corrupted by additive noise and multipath phenomena, and accurate TOA estimation. The classical acoustic pure tone pulse is compared with wide band coded spread spectrum signals (SS), resulting on improved TOA resolution and stronger multi-path and noise rejection.

The use of SS signals to be received by an USBL array of close-spaced hydrophones requires advanced signal processing techniques only available using a Digital Signal Processor. Therefore, system implementation must rely on real time digital signal processing techniques that allows for improved performance and versatility. Digital matched filter implementation is tackled based on the Discrete Fourier Transform (DFT) and its properties.

The overall performance of the proposed system is validated based on the results from a series of tests at sea.

1 Introduction

Acoustic positioning systems are designed with the purpose of tracking the evolution of an underwater vehicle or platform. These systems rely on the measurement of the times of arrival of an acoustic signal emitted by the moving target to a set of receivers with known positions. From TOA measurements bearing and/or range can be derived, and thus the position of the target.

Underwater Acoustic Positioning Systems are commonly used in a wide variety of underwater applications, including oil and gas exploration, ocean sciences, salvage operations, marine archaeology, law enforcement and military activities.

Acoustic positioning systems can achieve an accuracy of a few centimeters to tens of meters and can be used over operating distance from tens of meters to tens of kilometers. Performance depends strongly on the type and model of the positioning system, its configuration for a particular application, and the characteristics of the underwater acoustic environment at the work site.

1.1 Positioning systems architectures

Classical approches to underwater acoustic positioning systems are described in this section as presented in [17]. The distance between acoustic baselines (that is, the distance between the active sensing elements) is generally used to define an acoustic positioning system. In this way there are three primary types: Short Baseline (SBL), Ultra Short Baseline (USBL) and Long Baseline (LBL).

1.1.1 Short Baseline

In a SBL system a minimum of three receivers, about 20 to 50m apart, are installed in the hull of a surface vessel. From the detection of the acoustic signal and relative TOA measurements of different receivers a bearing is computed. If a time of flight interrogation technique is used (transducer$\leftrightarrow$transponder) a range to the emitter will also be available from the SBL system and thus a position can be derived.

Any range and bearing available from the SBL system is with respect to the receivers mounted on the vessel and, in this way, a SBL system needs additional tools such as vertical reference unit (VRU), gyroscope and surface navigation system (GPS) in order to provide a position on an Earth Reference System.

1.1.2 Ultra Short Baseline

Similar to SBL but here receivers are closely spaced (less than 50cm apart).

The close spacing of USBL receivers requires additional accuracy on TOA estimation. In this way, USBL systems rely on a phase difference or phase comparison of the acoustic signal between receivers, instead of the relative arrival time measurement.

Like in SBL systems a time of flight interrogation technique can be used to achieve a range to the emitter. Also the position derived from USBL systems is with respect to the receivers mounted on the vessel and therefore VRU,

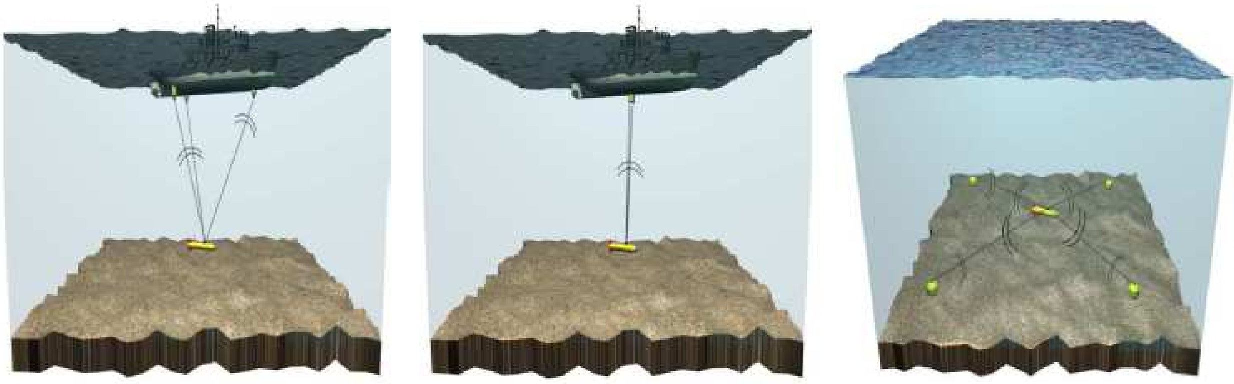

(a) SBL (b) USBL (c) LBL

Figure 1: Classical acoustic positioning systems architectures

gyroscope and GPS are needed to provide an Earth referenced position.

The main advantages of Short Baseline (SBL) and Ultra Sort Baseline (USBL) positioning systems are:

- Ship based systems (no need to deploy transponders on the seabed).
- Low system complexity makes SBL and USBL relatively easy tools to use.
- Good range accuracy with time of flight systems.

And the main disadvantages of these systems are:

- Detailed calibration of system is required.
- Absolute positioning accuracy depends on additional sensors (VRU and gyroscope).
- In the case of SBL system, large baselines (>40m) are needed for accuracy in deep water.

1.1.3 Long Baseline

A network of seabed transponders, with a baseline often several kilometers long, are deployed. The location of the baseline transponders either relative to each other or in global coordinates must then be measured precisely. A minimum of three transponders is needed but more may be used in order to introduce redundancy. Travel times are measured between the transponders and the vehicle to be tracked and position is calculated using triangulation techniques. Each transponder replies on a different frequency, thus allowing their signals to be distinguished from each other. The position derived from an LBL system is with respect to relative or absolute seabed coordinates and, unlike SBL and USBL, there is no need of additional components.

The main advantages of Long Baseline systems are:

- Very good position accuracy independent of water deep.
- High relative accuracy over large areas.

And the main disadvantages of this systems are:

- High system complexity
- Requires comprehensive calibration at each deployment.
- Operational time consumed for deployment/recovery.

2 Signal Processing and Positionig

In this section a comparison is made between two possible acoustic signals to be used by the underwater position system: the traditional sinusoidal tone burst; and a spread spectrum signal. The signal detection and time of arrival (TOA) estimation problems are studied and a solution is presented based on a matched filter. A closed-form method of estimating the transponder position in a reference coordinate frame is provided. The transponder distance and direction are obtained resorting to the planar approximation of the acoustic waves.

2.1 Signal detection and TOA estimation

The positioning system reciver has two principal functions. First it must detect if the expected signal is present in the water; if so it must then estimate the TOA of the signal. The direction and distance of the emitter are computated using the TOA measurments to different hydrophones and so the system requires accurate detection and TOA estimation of a known signal which may be corrupted by additive noise.

The optimal solution to a detection problem, from the point of view of signal to noise ratio (SNR), can be obtained resorting to the design of a matched filter, consisting of a linear system whose impulse response is a time reversed replica of the expected signal. The filter response is the correlation between the acquired and the expected signal. The arrival time correponds to the peak of the matched filter output.

For the TOA problem we can quantify the uncertainty of the estimation. The standard deviation for the TOA estimate is given by [2]:

$$\sigma_{TOA} \geq \frac{1}{BW\sqrt{\frac{2E}{n_0}}}, \tag{1}$$

where BW is a measure of the signal bandwidth and

$$\sqrt{\frac{2E}{n_0}} \tag{2}$$

is the SNR at the matched filter output where n_0 is the input noise level and E is the signal energy. From eq. 1 we see that there are two ways to reduce the TOA estimate variance and therefore improve the repeatability of the system: increasing the SNR; or increasing the bandwidth of the signal.

The classical signal used for underwater positioning is a narrowband tone burst, primarily because of the simplicity of the circuitry required to transmit and receive the signal. Let's see how can we reduce the TOA estimate variance for this particular signal.

In order to increase the SNR we must increase the energy of the received pulse E. For the sinusoidal signal the energy is proportional to amplitude and length. Signal amplitude is limited to transmitter power and therefore better SNR is achieved by sending a longer ping.

For the same type of signal the bandwidth is given by

$$BW = \frac{1}{T}, \tag{3}$$

where T is the pulse length, and so, to reduce the TOA estimate variance signal duration must be decreased.

From (1) and (3), and being $E \propto T$, the TOA estimation may be given that

$$\sigma_{TOA} \propto \sqrt{T}. \tag{4}$$

Equation (4) expresses a contradiction. When it is not possible to increase the transmitter power any further the signal must be lengthen in order to increase the SNR. This provides greater energy for detection but will also increase the TOA estimation variance which is not desirable. On the other hand, in order to achieve the highest possible timing resolution with a tone burst the optimal signal is as short as possible. However this causes that optimal signal to have too little energy to allow for reliable detection at long ranges.

Figure 2 shows the matched filter output for two sine pulses with different lengths. Both signals are corrupted by the same additive noise sequence.

With the shorter pulse shown in Fig. 2a a sharp peak is obtained in the filter output but with poor noise rejection. Figure 2b shows that when we lengthen the pulse, the noise rejection improves but the sharpness of the peak degrades.

The above discussion represents the ideal case where there is only one acoustic signal in the presence of additive white noise. In underwater acoustic however there are usually many multipaths, that are repllicas of the signal arriving later in time and at varying amplitudes caused by reflection. This kind of scenario often arises in shallow water channels where the signal is reflected from the sea surface (or seabed). Figure 3 shows the matched filter response to a sine pulse in the presence of a 2 ms delay and 75% amplitude multipath.

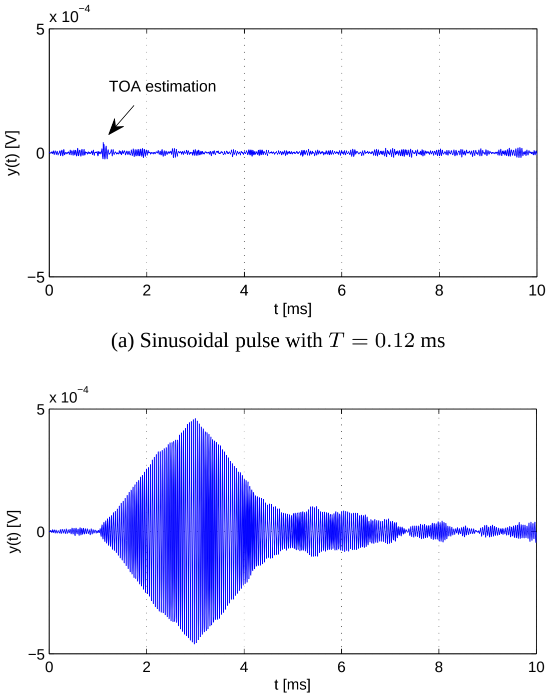

(a) Sinusoidal pulse with $T = 0.12$ ms

(b) Sinusoidal pulse with $T = 2$ ms

Figure 2: Matched filter output

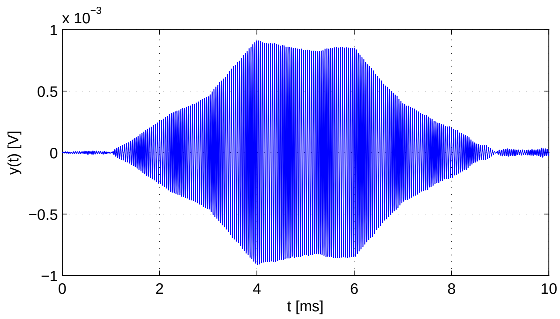

Figure 3: Matched filter output with multipath

Using a sine pulse, which has not a narrow autocorrelation peak, the response to the delayed signal is not well separated from the direct path.

We presented here the two main disadvantages of using a sine pulse.

- It is not possible to simultaneously increase range (SNR) and precision (decrease TOA estimation variance).
- Weak multipath rejection.

We can overcome these disadvantages by using a coded spread spectrum signal. SS signals are wideband signals whose autocorrelation function approaches an impulse. In addition with SS signals it is possible to maintain the bandwidth as pulse length is increased [2]. In this way, as we can see from (1), it becomes possible to increase signal energy by lengthening the SS pulse, increasing SNR and system range, and simultaneously reduce TOA estimation variance, improving system precision. Figure 4 illustrates the behaviour of the SS pulse under ideal conditions and corrupted by noise and multipath.

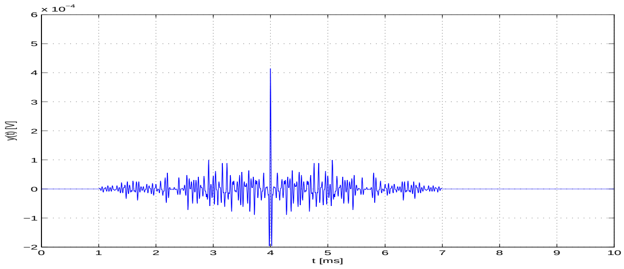

(a) SS signal under ideal conditions

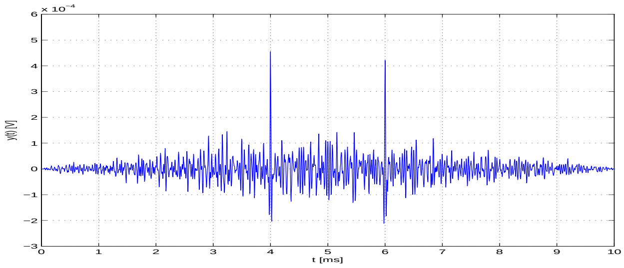

(b) SS signal corrupted by noise and multipath

Figure 4: Matched filter output

Figure 4 demonstrates that is possible, using a SS signal, to obtain a matched filter response whose noise rejection characteristics are similar to the long sine pulse, but whose sharpness is similar to the short one. Also in the presence of multipath the response to reflection and to the direct path is well separated allowing the detector to reliably find the first peak.

Although SS signal are relatively complex, the availability of low cost, high speed, Digital Signal Processors (DSP) now make it practical to consider using these waveforms in real world applications. From here on, and during the system development and testing, we will be using a SS acoustic signal.

2.2 Positioning

The direction and distance of the emitter are computed based on planar approximation of the acoustic wave. The problem is illustrated in fig. 5 with two receivers (i and k) projected on XY plan, a propagating plan wave, time of arrival to the receivers (t_i and t_k) and the unit direction vector of the emitter $\mathbf{d} = [\, d_x \; d_y \; d_z \,]^T$ with opposite sense and the same direction as the propagation vector.

The distance the planar wave travels between receivers i and k is given by

$$v_p(t_i - t_k) = -\mathbf{d}^T(\mathbf{r}_i - \mathbf{r}_k), \tag{5}$$

where v_p is the speed of sound in the water and $\mathbf{r}_i = [\, x_i \; y_i \; z_i \,]^T$, $\mathbf{r}_k = [\, x_k \; y_k \; z_k]^T$ the receivers positions on

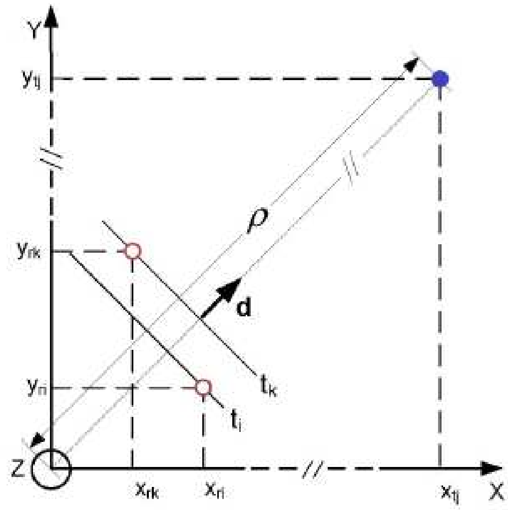

Figure 5: Planar wave approximation

Body frame. Without the use of vectorial notation eq. 5 becomes

$$v_p(t_i - t_k) = -(d_x(x_i - x_k) + d_y(y_i - y_k) + d_z(z_i - z_k)). \tag{6}$$

If there are N receivers there will be M equations like eq. 6 with $\{i = 1, \dots N \,; k = 1, \dots N \,; i \neq k\}$, being $M = {}^N_2C$ all possible combinations of the N receivers. The TDOA between the receivers,

$$\boldsymbol{\Delta} = [\Delta_1 \;\; \Delta_2 \;\; \dots \;\; \Delta_M]^T,$$

with $\Delta_1 = t_1 - t_2, \Delta_2 = t_2 - t_3, \dots \Delta_M = t_{N-1} - t_N$, can be generated by

$$\boldsymbol{\Delta} = \mathbf{C}\mathbf{t}_m,$$

where $\mathbf{C} \in \mathbb{R}^{M \times N}$ is a combination matrix and $\mathbf{t}_m = [t_1 \dots t_N]^T$ is the vector of time measurements from all receivers. In the same way, if we define for the receivers positions combinations

$$\mathbf{x} = [x_1 - x_2 \;\; x_2 - x_3 \;\; \dots \;\; x_{N-1} - x_N]^T,$$

$$\mathbf{y} = [y_1 - y_2 \;\; y_2 - y_3 \;\; \dots \;\; y_{N-1} - y_N]^T,$$

$$\mathbf{z} = [z_1 - z_2 \;\; z_2 - z_3 \;\; \dots \;\; z_{N-1} - z_N]^T,$$

the generalization of the problem for N receivers can be writen as

$$v_p\boldsymbol{\Delta} = -(d_x\mathbf{x} + d_y\mathbf{y} + d_z\mathbf{z}). \tag{7}$$

The least squares solution for the emitter's direction as presented in [3] is given by

$$\mathbf{d} = -v_p\mathbf{S}^{\#}\mathbf{C}\mathbf{t}_m, \tag{8}$$

where

$$\mathbf{S} = [\mathbf{x} \;\; \mathbf{y} \;\; \mathbf{z}] \qquad \text{e} \qquad \mathbf{S}^{\#} = (\mathbf{S}^T\mathbf{S})^{-1}\mathbf{S}^T.$$

Also resorting to the planar have approximation, the range of the emitter to the receiver i is given by

$$\rho_{ei} = v_p t_i, \qquad \text{with} \qquad i = 1, \dots N,$$

and the range to the origin of Body frame by

$$\rho_i = \rho_{ei} + \mathbf{d}^T \mathbf{r}_i, \tag{9}$$

where $\mathbf{d}$ is the previously computed emitter's direction vector.

By averaging the range estimates given by 10 for all the N receivers yields

$$\rho = \frac{1}{N} \sum_{k=1}^{N} \rho_i = \frac{1}{N} \sum_{k=1}^{N} (v_p t_i + \mathbf{d}^T \mathbf{r}_i). \tag{10}$$

3 System development

In this section we present the implementation done with focus on data acquisition and signal processing.

The USBL acoustic positioning system developed can be diveded into two parts: emission and reception. Building the emission box was not a purpose of this work and we used an existing box with the ability to generate a DSSS acoustic signal pre-recorded in memory. On the other hand, developing and programming the reception box was the main task to be done.

The heart of the reception box is the DSP that allows improved performance and versatility for the USBL acoustic positioning system. A TMS320C6713 floating-point DSP from Texas Instruments that operates at 225MHz was used. Before any DSP algorithm can be performed the signal must be in a digital form. This task is performed by a a 16 bit, 250 KSPS, 4 channel A/D converter. The system is controlled (start/stop, operation mode, data transfer, ...) by a host PC and the communication is ensured by a SMSC LAN91C111 Ethernet board.

The reception box electronics are mounted inside a rectangular splash-proof case with four hydrophone input connectors, a GPS antenna for PPS signal access, an external power supply and an Ethernet port. Emission box is shown on fig. 6.

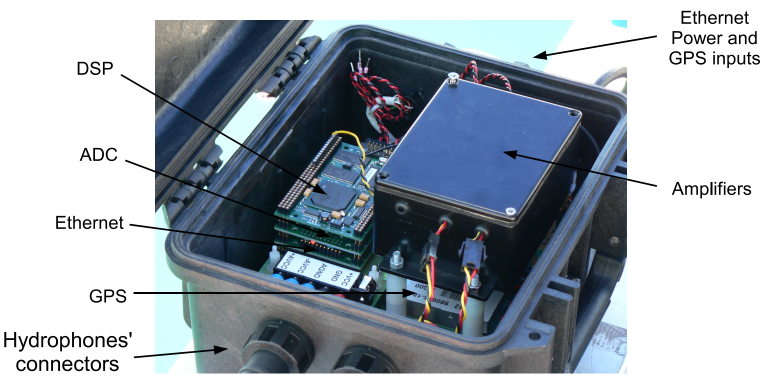

Figure 6: Reception box

3.1 Acquisition

This process starts with the array of 4 hydrophones, based on piezoelectric transducers that convert an acoustic wave into an electrical signal. The electric signals are then amplified by 4 variable gain amplifiers. These amplified analogue signals must be converted into a digital form. This process is performed by the ADC converter and involves the following steps: the signal is first sampled, converting the analogue signal into a discrete-time continuous amplitude signal; the amplitude of each signal sample is quantized into one of 2^{16} leves; the discrete amplitude levels are encoded into distinct 16 bit length binary words. This binary words, representing a digital form of the acoustic waves 'listened' by the hydrophones, must be temporarily stored in the DSP internal memory so that processing can be done to detect the presence of the expected signal and compute emitter's direction.

To tackle the digital data storage problem, a FIFO (first in first out) data buffer was implemented. The buffer is divided into blocks and while the ADC is acquiring new data the data present in the buffer is being processed. When the acquisition is completed the oldest block is replaced by the newest data and a new cycle begins. The number and length of the blocks is now the major concern. This is a delicate problem because during the time of one block acquisition, given by L/f_s where L is the block length and f_s the sampling frequency, the DSP must be able to process the data present in all blocks of the buffer. In this way the blocks must be large enough to give time for the data buffer processing but not too large because of memory constrains. This trade-off led us to use blocks of the same length L as the expected signal.

A sketch of the buffer hardware implementation is shown on Fig. 7 as well as the progress of an expected signal through the buffer. As the system has four hydrophones there will be four FIFO buffers for data storage, like the one in fig. 7.

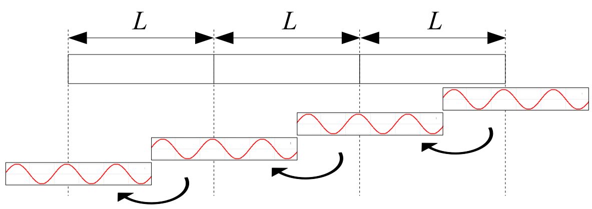

Figure 7: FIFO data buffer of length $3L$

When the system indicates the presence of the expected signal, it may be completely or just partially inside the buffer. Thus, in order to obtain accurate results, before estimate signal TOA to the different hydrophones and compute emitter position, we must be sure the expected signal is completely inside the buffer. The option of using three blocks of length L is because we want this to happen at least two times, and three is the minimum number of blocks that ensures that. Like this, the first detection is always ignored and just the second consecutive detection is accepted when is guaranteed that the signal is completely inside the buffer. At this time the acquisition is temporarily stoped to allow for TOA estimation and emitter's position computation.

It is important to remark that if just two L length blocks were used that would never be guaranteed.

3.2 Processing

In section 2.1 it was said that the use of a matched filter was the optimal solution for signal detection. Therefore a digital matched filter will be implemented in the DSP.

The digital filter output to a set of data $x[n]$ present in the buffer is given by the digital convolution (convolution sum) between $x[n]$ and the filter's impulse response $h[n]$

$$y[n] = (h \circledast x)\,[n] = \sum_{k=0}^{L-1} x[n-k]h[k]. \tag{11}$$

Because the matched filter purpose is to perform the correlation of the expected signal with the acquired data, it's impulse response $h[n]$ will be a replica of the expected signal sampled at the ADC working frequency f_s.

However convolution is a computational heavy operation. The standard convolution algorithm has quadratic computational complexity and, even with the use of fast digital signal processors its real-time computer implementation it is impossible in most applications. In this context it becomes important to introduce the concept of Discrete Fourier Transform (DFT) as correlation computation may be speeded up using DFT properties.

Let $\{x[n]\} = \{x[0], x[1], \ldots, x[N-1]\}$ be a sampled sequence, where N is the number of samples. Its Discrete Fourier Transform is the sequence of complex values $\{X[k]\} = \{X[0], X[1], \ldots, X[N-1]\}$ in the frequency domain, with the same length N, given by

$$X[k] = \sum_{n=0}^{N-1} x[n]e^{-jk\Omega nT}, \quad 0 \le k \le N-1, \tag{12}$$

where $\Omega = 2\pi/NT$ and T is the sampling period.

The inverse Discrete Fourier Transform (IDFT) restores the sequence $\{x[n]\}$ given its DFT $\{X[k]\}$ and it's defined by

$$x[n] = \frac{1}{N}\sum_{k=0}^{N-1} X[k]e^{+jk\Omega nT}, \ \ 0 \le n \le N-1. \tag{13}$$

The useful DFT property for correlation purposes is shown in Fig. 8. In a very simple way, we can say that it

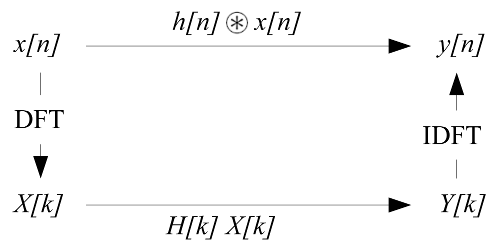

Figure 8: Convolution using DFT property

possible to 'change' a time domain convolution $h[n] \circledast x[n]$ for a frequency domain multiplication $H[k]X[k]$. This approach requires the computation of one DFT ($H[k]$ is permanently stored in the DSP internal memory), one multiplication and one IDFT, reducing computing complexity from $o(N^2)$ to $o(Nlog_2N)$. When the number of samples to be convolved is sufficiently large, as it is our case, this performance improvement, together with the use of a fast DFT algorithm (FFT), is extremely important because it makes real-time convolution implementation possible.

Even with the use of the above solution, convolution implementation can be further improved. As described in section 3.1 the data buffer consists of three memory blocks with same size L of the expected signal and, at the end of each acquisition cycle, just one of those blocks is renewed, being the other two just shifted. In this way it makes no sense to perform a $3L$ size convolution when just one third of the data is different from the previous acquisition cycle.

Let's consider the data buffer $3L$ length sequence $\{x[n]\}$ as a sum of three L length sequences, $\{x_1[n]\}$, $\{x[n]_2\}$ and $\{x[n]_3\}$, in the following way,

$$x[n] = \sum_{i=1}^{3} x_i[n-(i-1)L], \quad 0 \le n \le 3L-1, \tag{14}$$

with

$$x_i[n] = \begin{cases} x[n+(i-1)L], & if \quad 0 \le n \le L-1, \\ 0, & otherwise, \end{cases} \tag{15}$$

each sequence $\{x_i[n]\}$ representing the ith block of the data buffer. Replacing (14) in the matched filter output given by (11) yields

$$y[n] = \sum_{m=1}^{3} y_i[n-(i-1)L], \quad 0 \le n \le 4L-2, \tag{16}$$

where $y_i[n] = (h \circledast x_i)\,[n]$ is the filter's response to ith block's data.

As we can see from (16) it is possible to compute the convolution of the expected signal with the whole data buffer as a sum of the convolutions with each of the individual blocks. Thus, at each acquisition cycle we can perform a L size instead of a $3L$ size convolution, considerably improving time performance. This convolution method is known as overlap-add because since each $h \circledast x_i$ convolution has length $2L-1$ there will be an overlap of $L-1$ elements when adding $h \circledast x_1$ to $h \circledast x_2$ and $h \circledast x_2$ to $h \circledast x_3$.

3.3 Decision

After performing the matched filter convolution the system has to decide if the expected signal is or not present in the data buffer. To study the decision criterion we should look back to figures 4a and 4b where the filter's response to a DSSS signal was presented.

The idea behind the decision criterion will be to compare the maximum value of the matched filter's output with its average absolute value. Because of the noise, that is an unknown component of the acquired data, there will always be some degree of uncertainty. However, since having a maximum value considerably higher than the average absolute value is a characteristic associated with the filter's response to the expected DSSS sigal and not to the noise, we will consider that the greatest the difference between those two values, the greatest the chance that the expected signal is present in the buffer.

In this way we define a threshold for the system, and the expected signal is considered to be present when

$$\frac{max\,\{y[n]\}}{avg\,\{|y[n]|\}} > threshold. \qquad (17)$$

When the expected signal presence is indicated the system has to wait for the next acquisition cycle and just the second consecutive detections guarantees that the signal is completely inside the buffer, as explained in section 3.1.

3.4 Position computation

Unlike acquisition, that is continually happening for all the four hydrophones, the processing of the acquired data and signal presence decision are implemented just for one of the four hydrophones. We remeber that the whole processing and decision must be performed in less time than one buffer block acquisition, being this the most critical point of implementation. For this reason it is not possible to process the data present in all the four buffers. Despite this, when the expected signal is detected in the data buffer chosen for real-time processing, acquisition is temporarily interrupted and the three left data buffers are processed in order to find signal TOA. Position is computed according to the study presented in section 2.2, after what acquisition is restarted.

4 At sea tests

Once the implementation was completed a series of at sea tests were conducted. Tests took place in Cidade da Horta, Açores, between June 22 and 26, 2009.

Since position result is expressed in USBL array's coordinate frame it is desirable that the array remains at rest relative to Earth's coordinate frame, otherwise USBL array's movement would influence position computation even when emitter's position is stationary. For this reason tests were hold inside an harbor. Like this it was possible to firmly fasten the array ensuring that position results were not influenced by its movements. However multipath and noise presence is much stronger inside the harbor and tests results were affected by this.

Tests are divided into two categories: stationaty and dynamic. In both of them results' analysis is carried out separately for distance and direction estimation because computation methods are different, as seen in section 2.2.

4.1 Stationary tests

For stationary tests the emitter was tied to a pier that suffers negligible fluctuations for the purpose intended and the system was left running for 20 minutes. The histogram of stationary distance results, as obtained during the test by DSP processing, is presented in Fig. 9.

From Fig. 9 we see that distance results are mostly divided between two non-contiguous sub-intervals,

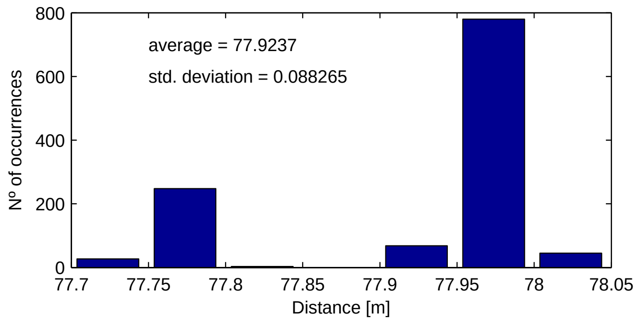

Figure 9: Histogram of stationay test distance results

$[77.70; 77.80]m$ and $[77.90; 78.05]m$. Being the emitter and the USBL array both stationary this is an unexpected result. In order to understand the reason why it happens we should look to the data used to decide about the presence of the signal and to compute emitter's distance. Matched filter convolution for two different detections is shown in Fig. 10.

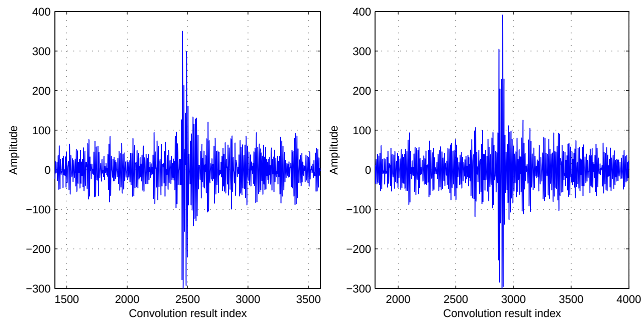

(a) Direct path detection (b) Indirect path detection

Figure 10: Matched filter convolution

As can be seen from Figures 10a and 10b matched filter convolution has two maximums very close in value. Because signal TOA is computed as the convolution's peak, when the absolute maximum is the first one distance will lie at the nearest sub-interval and when the absolute maximum is the second one distance will lie at the farthest sub-interval.

After a detailed analysis of convolution results of the four channels for all detections we can say that Figures 10a and 10b are representative of what happened throughout the test. In Fig. 11 it is presented an histogram of the time difference between the two convolution maximums for the different channels.

As it is clearly shown in Fig. 11 the time difference between the two convolution maximums varies from channel to channel. That difference is greater for channel 4 convolutions, smaller for channel 3 and intermediate for channels 1 and 2. Taking into account the above remarks and knowing that to channel 4 is connected the deepest hydrophone, to channel 3 the hydrophone closest to the surface and to channels 1 and 2 the hydrophones at intermediate depth, we find that the second maximum in the matched filter convolution is caused by a signal reflection on the sea surface, being the first maximum caused by di-

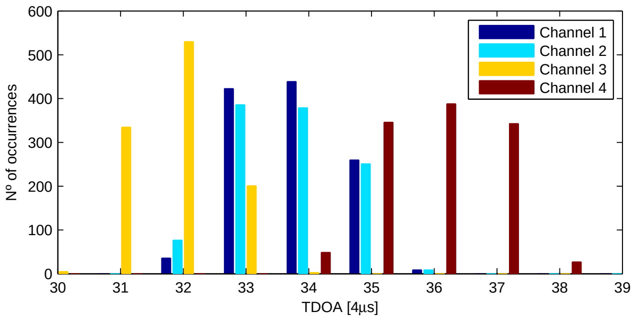

Figure 11: Histogram of the time difference between the two convolution maximums

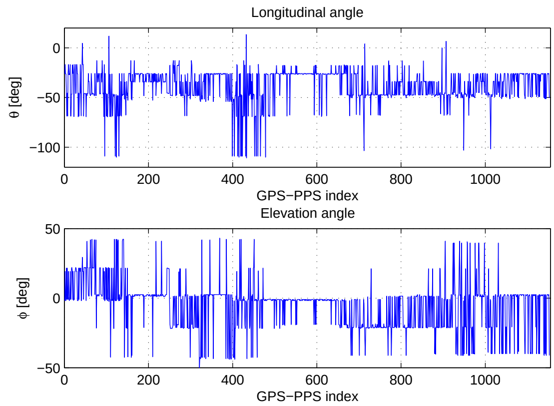

Figure 13: Stationay test direction results

rect path signal arrival.

To get round this multipath detection problem we have to modify TOA estimation method. When the decision criterion given by (17) is true, instead of estimate TOA as the absolute maximum position, we will consider TOA to be given by the position of the first maximum that exceeds the decision threshold. In Fig. 12 we reproduce the results presented before in Fig. 9, obtained now post-processing the data acquired during the test with the new TOA estimation method.

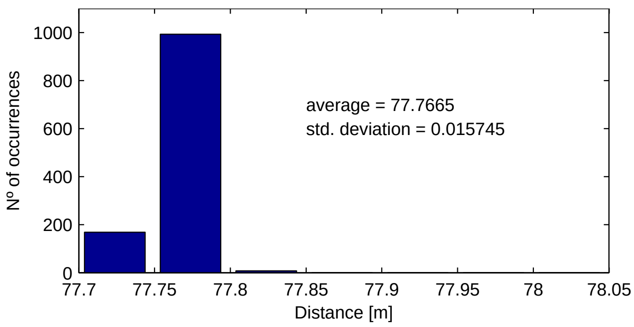

Figure 12: Histogram of stationay test distance results with new TOA estimation method

As can be seen from Fig. 12, with the new TOA estimation method, distance results are no longer divided between two non-contiguous sub-intervals and distance standard deviation is reduced form 8.8 to 1.6cm. In this way system rejection to multipath is greatly improved and therefore global system performance.

If multipath effects have caused errors in the order of centimeters when computing emitter's distance, when computing emitter's direction those erros are in the order of tens of degree. The stationary direction results, as obtained during the test by DSP processing, are plotted in Fig. 13.

As can be seen from Fig. 13 direction computation gave very inconsistent results.

However, in order to understand the reason of this poor performance, it's better to look to the data used to compute emitter's direction than to the final result. As described in section 2.2 direction is computed from signal TDOA to the different hydrophones. In Fig. 14 we present 3 histograms of TDOA between the 4 hydrophones.

We see that inconsistent direction results shown in Fig. 13 are justified by inconsistent TDOA estimation presented in Figures 14a, 14b and 14c. As previously happened in distance computation (Fig. 9), TDOA results are divided between non-contiguous sub-intervals. Also the time difference between those sub-intervals, 30 to 40 samples, is similar (see Fig. 11) suggesting that the problem may be caused by signal reflection as before. Therefore, we will try to solve the problem in the same way: modify TOA estimation method to avoid multipath detection. In Fig. 15 we reproduce the results presented in Fig. 14, obtained now post-processing the data acquired during the test with the new TOA estimation method.

As expected, new TOA estimation method greatly improves TDOA estimation, which has now a precision of about $8\mu s$ (2 samples). Emmiter's direction computed with this TDOA data is shown in Fig. 16. Comparing it with direction obtained during the test (Fig. 13) becomes evident that system performance is drastically enhanced, being both angles estimated with a standard deviation of about 0.4 deg.

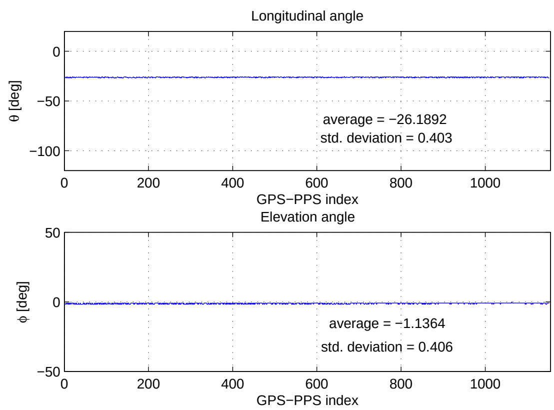

Figure 16: Stationay test direction results with new TOA estimation method

When it comes to time delay estimations there is a very common method: cross-correlation between data. With the purpose of finding signal TDOA to different hydrophones, cross-correlation was also employed in post-processing analysis. Obtained results are not presented

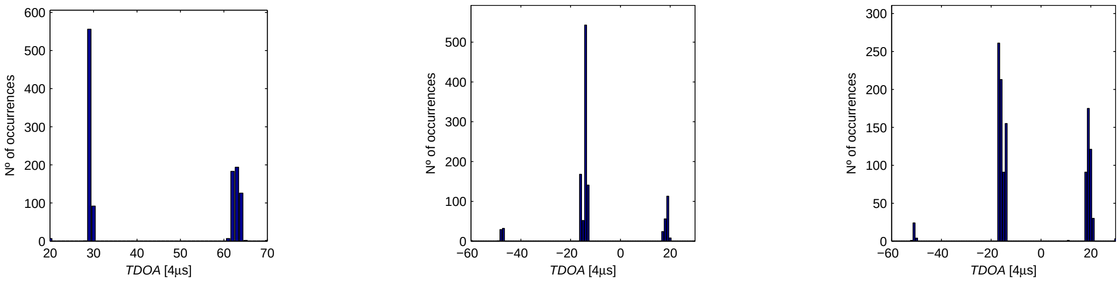

(a) TOA1 - TOA2 (b) TOA1 - TOA3 (c) TOA1 - TOA3

Figure 14: TDOA histograms of stationary test direction results

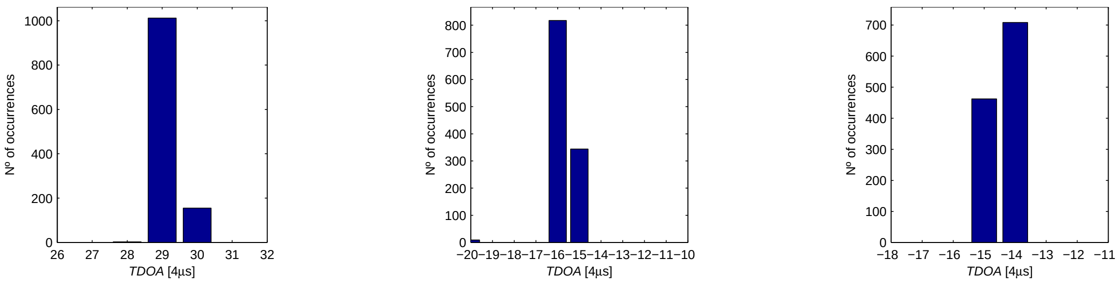

(a) TOA1 - TOA2 (b) TOA1 - TOA3 (c) TOA1 - TOA3

Figure 15: TDOA histograms of stationary test direction results with new TOA estimation method

here but they revealed an interesting feature: cross-correlation performance depends on the channels being processed. Similar performance is achieved for TOA1-TOA2 estimation (channels 1 and 2 are connected to hydrophones at the same depth) and inferior performance for any other two channels. This result is also justified by signal reflection and hydrophone placement at different depths.

4.2 Dynamic tests

For dynamic test the emitter was installed in a boat whose position was being recorded using a GPS. The distance and angles intervals that was possible to test were very limited. Still, dynamic test was conducted inside the harbor to allow adequate fastening of USBL receiving array, like explained in the begining of the section.

Dynamic test duration was 1445 s (approximately 24 min). Since emisson frequency is one signal per second, 1445 would be the maximum number of detections. However, 203 emissions were lost (14% of total). In Fig. 17 distance results for dynamic test are shown. Lost emissions are plotted at 0 m distance.

In addition to lost emissions there are detections that lead to clearly incorrect distance results. These incorrect results are caused by direct path signal lost and correspondent multipath detection. In order to quantify these cases we consider a maximum speed of $4 m.s^{-1}$ for the boat and a particular distance result is classified as incorrect if it means a higher speeed since the last detection. In this way, from 1242 detections 1210 are classified as correct (84% of 1445 total emissions). Given the percentages of

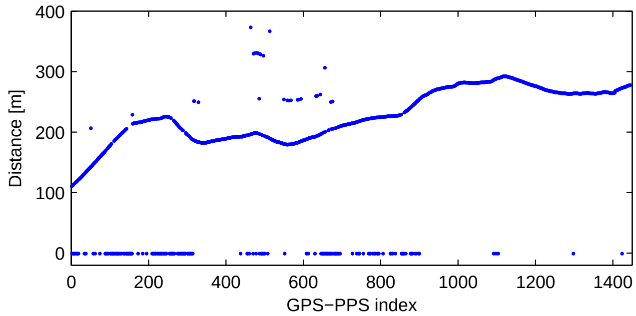

Figure 17: Dynamic test distance results

detections and results classified as correct, dynamic distance computation performance is considered satisfactory.

To assess system performance computing emitter's direction we follow the same strategy. Direction results are not plotted but percentage of correct results is presented in Table 1. We compare direction results obtained with two different methods for TDOA estimation already mentioned: first convolution maximum that exceeds decision threshold and data cross-correlation. Just the 1210 receptions that led to a correct distance result are used now.

	θ	ϕ
Matched filter peak	822 (68%)	866 (72%)
Cross-correlation	986 (81%)	1007 (83%)

Table 1: Dynamic test direction results

Both methods lead to similar performance but, unlike stationary test, cross-correlation presents slightly better results now. Also performance is very similar between longitudinal and elevation angles. This fact can be questioned since, as we said before, cross-correlation method performance depended on the channels being processed and that performance was considerably better for TOA1-TOA2 estimation, channels connected to hydrophones at the same depth and therefore sufficient to compute longitudinal angle. However, in section 2.2 we developed a least squares solution for emitter's direction that uses all the 4 channels to compute any of the angles. Like this it is possible to increase redundancy but also the inferior performance estimating TDOA for hydrophones placed at different depths can be damaging longitudinal angle computation. To confirm that we repeat direction computation, now without least square minimization and using channels 1 and 2 (same depth) to calculate longitudinal angle and channels 3 and 4 (different depths) for elevation angle.

	θ	ϕ
Matched filter peak	1121 (93%)	902 (75%)
Cross-correlation	1203 (99%)	1008 (83%)

Table 2: Dynamic test direction results without least squares minimization

From Table 2 we see that again cross-correlation presents slightly better results, but performance between longitudinal and elevation angles is now quite different. Longitudinal angle performance significantly improves, approaching 100% of correct results, and elevation angle performance remains at the same accuracy level. These results show that least square minimization was damaging system performance. Separating channels 1 and 2 from 3 and 4 we lose redundancy but the less accurate TDOA estimation from channels 3 and 4 is not damaging longitudinal angle computation. Nevertheless, least square minimization should be a good option when TDOA estimation error is similar between channels.

To give a global idea of system potential we compare in Fig. 18 emitter's GPS tracking with USBL positioning computed from correct distance results and longitudinal angle obtained without least squares minimization.

5 Conclusions

This work presented the design, implementation, and validation at sea of an USBL acoustic positioning system.

Signal detection and TOA estimation were based on the matched filter response, which leads to the highest signal-to-noise-ratio. The classical acoustic pure tone pulse was compared with wide band coded spread spectrum signals, resulting on improved TOA resolution and stronger multipath and noise rejection. Emitter's position is computed resorting to the planar approximation of the acoustic wave.

The most critical development task was digital filter implementation. Digital filtering consists of signal convolution and must be performed within practical time. Real time implementation was possible thanks to the use of a

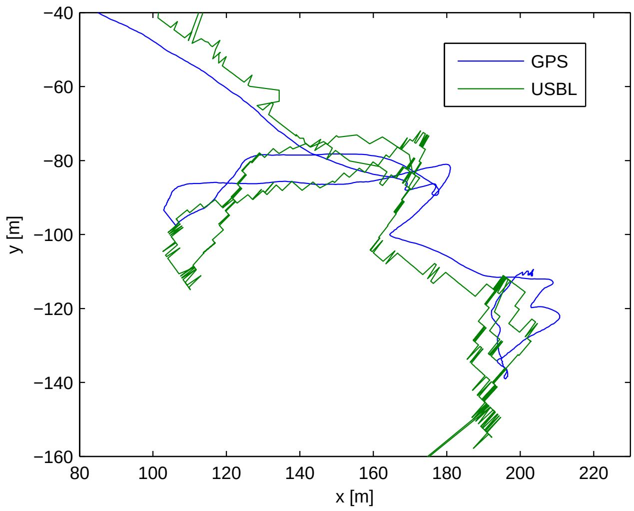

Figure 18: GPS vs. USBL positioning

DSP and processing techniques that greatly reduce convolution time (based on DFT properties).

Validation tests were conducted inside an harbor for being possible to firmly fasten the USBL array ensuring that position results were not influenced by its movements. However multipath and noise presence are much stronger inside the harbor which strongly affected tests results. Throughout the test signal surface reflection made accurate TOA estimation difficult and, therefore, accurate distance and direction computation. A slight change in TOA estimation method was proposed (first maximum that exceeds the decision threshold instead of absolute maximum position) and post-processing results evidenced that system rejection to multipath was greatly improved which led to improved accuracy in distance and direction computation. From dynamic test results analysis we saw that TDOA estimation accuracy depended on the channels being processed and, for this reason, it was advantageous to give up from least squares minimization in direction computation, losing redundancy but isolating less accurate TDOA estimations.

References

[1] A. Alcocer, P. Oliveira, and A. Pascoal. Underwater Acoustic Positioning System Based On Buoys With GPS. *Proceedings of the Eighth European Conference on Underwater Acoustics, 8th ECUA*, June 2006.

[2] Thomas C. Austin. The Application of Spread Spectrum Signaling Techniques to Underwater Acoustic Navigation. *Proceedings of the 1994 Symposium on Autonomous Underwater Vehicle Technology*, 1994.

[3] P. Batista. Controlo de Veículos Autónomos Baseado na Informação Directa de Sensores Acústicos. Relatório de trabalho final de curso, Universidade Técnica de Lisboa - Instituto Superior Técnico, Setembro 2005.

[4] R. Cusani. Performance of Fast Time Delay Estimators. *IEEE Transactions on Acoustics, Speech, and Signal Processing*, vol. 37(5):757–759, May 1989.

[5] F. Gustafsson and F. Gunnarsson. Positioning Using Time-Difference Of Arrival Measurements. *Proceedings of the IEEE International Conference on Acoustics, Speech, and Signal Processing*, 2003.

[6] Emmanuel C. Ifeachor and Barrie W. Jervis. *Digital Signal Processing. A Practical Approach*. Addison-Wesley Ltd., 7th edition, 1998.

[7] Sonardyne Inc. http://www.sonardyne.com/, 2009.

[8] F. Lima and C. M. Furukawa. Development and Testing of an Acoustic Positioning System - Description and Signal Processing. *Proceedings of the IEEE 2002 Ultrasonics Symposium*, 2002.

[9] Isabel M. G. Lourtie. *Sinais e Sistemas*. Escolar Editora, 2nd edition, 2007.

[10] P. H. Milne. *Underwater Acoustic Positioning Systems*. Gulf Publishing Company, 1983.

[11] Sanjit K. Mitra. *Digital Signal Processing. A Computer-Based Approach*. McGraw-Hill, 2nd edition, 2001.

[12] M. Morgado, P. Oliveira, C. Silvestre, and J. F. Vasconcelos. USBL/INS Tightly-Coupled Integration Technique for Underwater Vehicles. *Proceedings Of The 9th International Conference on Information Fusion*, 2006.

[13] Marco M. Morgado. Sistema de Navegação Inercial com Ajuda USBL. Relatório de trabalho final de curso, Universidade Técnica de Lisboa - Instituto Superior Técnico, Setembro 2005.

[14] J. O. Smith and J. S. Abel. The Spherical Interpolation Method of Source Localization. *IEEE Journal of Oceanic Engineering*, vol. 12(1):246–252, 1987.

[15] D. Thomson and S. Elson. New Generation Acoustic Positioning Systems. *Oceans 2002*, vol. 3:1312–1318, Oct. 2002.

[16] Robert J. Urick. *Principles of Underwater Sound*. Peninsula Publishing, 3rd edition, 1983.

[17] K. Vickery. Acoustic Positioning Systems. A Pratical Overview Of Current Systems. *Proceedings of the 1998 Workshop on Autonomous Underwater Vehicles*, August 1998.

[18] K. Vickery. Acoustic Positioning Systems. New Concepts - The Future. *Proceedings of the 1998 Workshop on Autonomous Underwater Vehicles*, August 1998.

[19] J. Yli-Hietanem, K. Kalliojarvi, and J. Astola. Low-Complexity Angle of Arrival Estimation of Wideband Signals Using Small Arrays. *Proceedings Of The 8th IEEE Signal Processing Workshop on Statistical and Array Processing*, 1996.